TURBULENCE MODELLING OF HIGH-PRESSURE CONVECTIVE BOILING TWO-PHASE FLOWS

J. Guéguen¹, F. François¹ and H. Lemonnier¹

¹ DTN/SE2T, Commissariat à l'Energie Atomique, Grenoble, 38054, France jil.gueguen@cea.fr, fabrice.francois@cea.fr, herve.lemonnier@cea.fr

Abstract

This article is a contribution to the modelling of multidimensional high-pressure convective boiling two-phase flows relative to PWR's thermal hydraulics conditions.

Postulating that the turbulence is one possible physical mechanism for heat removal from the wall towards the two-phase flow core, this work focuses on modelling turbulent transport terms in the momentum and energy balance equations.

Using the pioneering work of Sato *et al.*, [1], [2], the momentum and the energy balance equations are derived for a two-phase mixture. Such a system can be expressed as a combination of parameters, which include the local void fraction as well as the fluid velocity profile, the wall shear stress and the eddy diffusivity. By specifying a closure relation for this last parameter, a numerical solution can be obtained. As a preliminary step towards a numerical solution, the turbulent structure of the two-phase flow is expressed as a linear superposition of an inherent liquid turbulence and an additional one due to the bubble agitation. On the basis of this theory, the mixture velocity and temperature profiles can be predicted provided that the local void fraction and the wall shear stress are known.

The model is then tested against the experimental data bank DEBORA (Garnier *et al.*, [3]) which is devoted to the study of high pressure boiling flows. The first results are encouraging for the mechanical part but some discrepancies are observed on temperature profiles for boiling tests. This work should be continued in order to (i) improve the model especially for the thermal aspects and (ii) identify the key parameters responsible for the heat flux limitation (DNB).

Keywords: Turbulence, two-phase flow, high pressure, convective flow

1. Introduction

To predict momentum and heat transfer process in boiling flows, it appears of great importance to characterize the turbulent structure of two-phase flow. The purpose of this paper is to develop a method to access the turbulent fluxes from the balance equations and the flow characteristics provided by the data bank DEBORA. In a first step, turbulent fluxes terms are compared to the eddy viscosity model of Sato *et al.*, [1], [2]. As a future work, these fluxes will be compared to more complex models such as k-epsilon or R-ij-epsilon currently used in CFD codes. These models have been developed and tested for adiabatic air-water two-phase flows but their validity for PWR's conditions is not clearly established.

2. Theory – Model development

The physical model proposed in this paper is based on the work of Sato *et al.*, [1], [2]. The theory describes transfer process of momentum and heat in a two-phase bubbly flow. The present study is concerned with two-dimensional two-phase flow in a vertical pipe. The coordinate system is shown in figure 1.

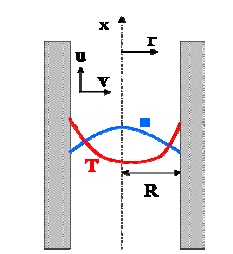


Figure 1 Flow parameters

2.1 Momentum transfer

First, let us express the local time-averaged balance equation of momentum for the two-phase flow mixture. The following assumptions are made: the flow is stationary and sufficiently developed so that convective term can be neglected. According to Ishii [4], it can be written:

$$\underline{g}\rho_m - \underline{\nabla}p_m + \underline{\nabla}\underline{\tau}_m = 0 \tag{1}$$

where ρ_m , p_m et τ_m are respectively the mixture density, the mixture pressure and the mixture stress tensor and can be expressed as:

$$\begin{cases}
\rho_{m} = \sum_{k=L,G} \alpha_{k} \overline{\rho_{k}}^{X} \\
p_{m} = \sum_{k=L,G} \alpha_{k} \overline{p_{k}}^{X} \\
\underline{\underline{\tau}_{m}} = \sum_{k=L,G} \alpha_{k} \underline{\underline{\tau}_{k}}^{X}
\end{cases} \tag{2}$$

 $\overline{f_k}^x$ is defined as follows:

$$\overline{f_k}^X = \frac{1}{T_k} \int_{T_k} f_k dt \tag{3}$$

By projecting equation (1) on the x-axis, and integrating it from 0 to r, we obtain:

$$r\tau_m(r) = \frac{\partial p_m}{\partial x} \frac{r^2}{2} + g \int_0^r \rho_m(r) r dr$$
 (4)

The pressure gradient is assumed to be independent from the radial coordinate. For r=R, the equation (4) can be rewritten:

$$R\tau_{m}(R) = \frac{\partial p_{m}}{\partial x} \frac{R^{2}}{2} + g \int_{0}^{R} \rho_{m}(r) r dr$$
 (5)

Combining (4) and (5) leads to:

$$\tau_{m}(r) = -\frac{r}{R}\tau_{w} + \frac{g}{r}\int_{0}^{r} \left(\rho_{m}(r) - \left\langle \rho_{m}(r) \right\rangle_{2}\right) r dr \tag{6}$$

where: $\langle \rho_m(r) \rangle_2 = \frac{1}{\pi R^2} \int_0^R \rho_m(r) 2\pi r dr$ and $\tau_m(R) = -\tau_w$ (τ_w is the wall shear stress)

2.2 Heat transfer

Starting from the local time-averaged total energy balance equation for the mixture, the following assumptions are considered: the flow is steady, gravitational and viscous terms are neglected and the density of each phase is spatially uniform. Under these assumptions, the balance equation can be written (Ishii [4]):

$$\underline{\overrightarrow{\nabla}}.\sum_{k} \left[\alpha_{k} \rho_{k} \overline{h_{k}}^{X} \underline{\underline{V_{k}}}^{X} \right] = -\underline{\nabla}.\sum_{k} \alpha_{k}.(\underline{\underline{q_{k}}}^{X} - \rho_{k} \overline{h_{k}} \underline{V_{k}}^{X})$$

$$(7)$$

where $\overline{f_k}^x$ is defined by:

$$\overline{\overline{f_k}}^X = \frac{\overline{\rho_k f_k}^X}{\overline{\rho_k}^X} \tag{8}$$

Turbulent decomposition is defined by:

$$\begin{cases}
h_k = \overline{h_k}^X + h_k' \\
\underline{\underline{V}_k} = \underline{\underline{V}_k}^X + \underline{\underline{V}_k}'
\end{cases}$$
(9)

We assume now that (i) there is no heat transfer in the vapor phase which will be supposed at

saturation and (ii) the heat is only transported by liquid phase, so equation (7) can be rewritten:
$$\underline{\nabla}.\sum_{k} \left[\alpha_{k} \rho_{k} \overline{h_{k}}^{X} \underline{\underline{V}_{k}}^{X} \right] = -\underline{\nabla}.\alpha_{L}.\left(\underline{\underline{q}_{L}}^{X} - \rho_{L} C_{pL} (T_{L}) \overline{T_{L}' \underline{V}_{L}'}^{X}\right)$$
(10)

with $h_L' \approx C_{pL}(T_L)T_L'$, C_{pL} is the heat capacity at constant pressure of liquid (J/kg).

We now assume that the averaged phase enthalpy $\overline{h_h}^x$ can be decomposed as follow:

where $H_m(x)$ is the mean enthalpy given by the one dimensional total energy balance equation:

$$\dot{M} \frac{d}{dx} H_m(x) = 2\pi R q_w$$
 (12)

where \dot{M} is the total mass flow rate and q_w is the wall heat flux.

 $h_{\nu}(r)$ is the radial profile of enthalpy which is assumed to depend only on the radial coordinate. By combining (10) and (11), we obtain:

$$\frac{\partial}{\partial x} \left(H_m(x) \sum_{k} \left[\alpha_k \rho_k u_k \right] \right) = -\frac{1}{r} \frac{\partial}{\partial r} \left(r \alpha_L Q_L(r) \right) \tag{13}$$

where u_k is the axial component of \underline{V}_k and $Q_L(r)$ is the total heat flux defined by:

$$Q_L(r) = \overline{\overline{q_{Lr}}}^{X} - \rho_L C_{pL}(T_L) \overline{\overline{T_L' v_L'}}^{X}$$
(14)

We have assumed the convective term was essentially axial whereas the diffusive term (right member of equation (10)) is essentially radial.

By combining equation (12) and (13) and after integrating the equation, we finally obtain:

$$Q_L(r) = -\frac{q_w"}{\alpha_L(r)} \frac{R}{r} \frac{\dot{M}(r)}{\dot{M}}$$
(15)

where $\dot{M}(r)$ is given by:

$$\dot{M}(r) = \int_{0}^{r} 2\pi r G(r) dr \tag{16}$$

If we moreover make the assumption of flat profiles, equation (15) simplifies in:

$$Q_L(r) = -\frac{q_w"}{\alpha_L(r)} \frac{r}{R}$$
 (17)

Supposing $\alpha_L \approx 1$, equation (17) simplifies to equation [32] in Sato *et al.*'s paper [2].

2.3 Closure relation of turbulent transport term

2.3.1 Turbulence and boundary layer approximation

For turbulent single-phase flows, within the quasi develop flow assumption, the shear stress and the heat flux normal to the main flow direction can be expressed as:

$$\begin{cases}
\tau_{tot} = \rho v \frac{\partial \overline{u}}{\partial r} - \rho \overline{u'v'} \\
q_{tot} = -\left(k \frac{\partial \overline{T}}{\partial r} + \rho C_p \overline{v'T'}\right)
\end{cases}$$
(18)

The first term on the right side is due to molecular diffusion and the second term is due to turbulent mixing. υ is the kinematic viscosity, k the thermal conductivity, C_p the heat capacity, u', v', T' are relative to the turbulent component of these quantities and $\overline{(.)}$ means time-averaged quantities.

2.3.2 Eddy viscosity concept

A simple conceptual model for turbulent flow deals with eddies which are small portions of fluid in boundary layer that move about for a short time before losing their identity. Similarly to the contribution due to molecular diffusion, the transport coefficient, which is defined as eddy diffusivity for momentum transfer ε_M (m²/s) and for heat transfer ε_H , may be expressed as:

$$\begin{cases}
\varepsilon_{M} \frac{\partial \overline{u}}{\partial r} = -\overline{u'v'} \\
\varepsilon_{H} \frac{\partial \overline{T}}{\partial r} = \overline{v'T'}
\end{cases}$$
(19)

Based on this model, we may assume a similar relation to express the shear stress distribution of a mixture (equation (6)):

$$\tau_{m}(r) = \rho_{m}(\nu_{m} + \varepsilon_{M}) \frac{\partial u_{m}}{\partial r} \approx \rho_{m}(\nu_{L} + \varepsilon_{M}) \frac{\partial u_{m}}{\partial r}$$
(20)

where v_m is the "mixture viscosity", which will be approximated in this study by the liquid viscosity v_L . Similarly equation (17) can be written as:

$$Q_{L}(r) = -(k_{L} + C_{PL}\rho_{L}\varepsilon_{H})\frac{\partial \overline{T_{L}}}{\partial r}$$
(21)

2.3.3 Sato *et al.* model [1]

To predict momentum and heat transfer process of bubbly flow, it is of importance to understand turbulent structure of continuous liquid phase, which may result in how to describe the contribution of bubble influence to flow characteristics. Sato *et al.*, [1], have proposed an analysis in which turbulent shear stress in bubbly flow is linearly subdivided further into two

components, one due to the liquid flow turbulence and an other due to an additional turbulence caused by bubble agitation:

$$\varepsilon_{M} = \varepsilon' + \varepsilon'' \tag{22}$$

where ϵ ' and ϵ '' are respectively the eddy diffusivity for single-phase turbulent flow and the eddy diffusivity due to bubbles. If we admit the Prandtl analogy, the eddy diffusivity of momentum ϵ_M will be equal to the energy eddy diffusivity ϵ_H .

 ε ' is modeled by the Reichardt formula [5], which is valid for the core flow region, corrected by a damping A factor supposed to be suitable in the vicinity of the wall.

$$\varepsilon'(r) = A \frac{kR}{6} \sqrt{\frac{\tau_w}{\rho_L}} \left[1 - \left(\frac{r}{R}\right)^2 \right] \left[1 + 2\left(\frac{r}{R}\right)^2 \right]$$
 (23)

k=0.4 is the Kármán constant, τ_w is the wall shear stress and A is expressed as:

$$A = \left[1 - \exp\left(-\frac{(R - r)}{16\nu_L} \sqrt{\frac{\tau_w}{\rho_L}} \right) \right]^2 \tag{24}$$

Sato et al. [1] propose for ε " the following closure relation which is assumed to take into account the influence of bubbles in the liquid flow:

$$\varepsilon''(r) = Ak_1 \alpha_G(r) \frac{d_b(r)}{2} \hat{U}_b$$
 (25)

A is the damping factor, k_1 =1.2 an empirical constant, $d_b(r)$ the radial distribution of the mean bubble diameter and \hat{U}_b the cross-sectional mean relative velocity. For taking into account the reduction of bubble size towards the wall, Sato *et al.* [1] propose this expression for bubble $d_b(r)$:

$$d_{B}(r) = \begin{cases} \hat{d}_{B} & 0 \le r \le R - \hat{d}_{B}/2 \\ 4(R-r)(\hat{d}_{B}+r-R)/\hat{d}_{B} & R - \hat{d}_{B}/2 \le r \le R - 20\mu m \\ 0 & R - 20\mu m \le r \le R \end{cases}$$
(26)

 \hat{d}_{B} is the cross-sectional mean diameter of bubbles. As Sato *et al.* [1] do not mention how is calculated \hat{U}_{b} , we have chosen to evaluate this relative velocity by using the mean drift velocity in bubbly flow given by Ishii [6]:

$$\hat{U}_b = \sqrt{2} \left(\frac{g \sigma \Delta \rho}{\rho_L^2} \right)^{\frac{1}{4}} (1 - \langle \alpha_G \rangle)^{1.75}$$
(27)

 σ is the surface tension (N/m), $\Delta \rho = \rho_L - \rho_G$, $\langle \alpha_G \rangle$ is the cross-sectional mean void fraction.

3. Numerical calculations

3.1 Velocity distribution

For a prescribed mass flow rate G, if the void fraction profile $\alpha(r)$ is specified, the mixture velocity distribution $u_m(r)$ and the wall shear stress τ_w can be calculated numerically. Equations (6) and (20) lead to:

$$\frac{du_{m}}{dr} = \frac{-\frac{r}{R}\tau_{w} + \frac{g}{r}\int_{0}^{r} (\rho_{m}(r) - \langle \rho_{m}(r) \rangle_{2})rdr}{\rho_{m}(\nu_{L} + \varepsilon_{M})}$$
(28)

The numerical procedure for solving equation (28) is shown in figure 2a.

3.2 Liquid temperature distribution

Equations (17) and (21) lead to the following expression for the liquid temperature radial profile:

$$\frac{\partial \overline{T_L}}{\partial r} = \frac{\frac{q_w"r}{\alpha_L(r)R}}{(k_L + C_{PL}\rho_L\varepsilon_H)}$$
(29)

Similarly, if the wall heat flux q_w " and the bulk liquid temperature T_{Lb} are given, heat transfer problem can be solved numerically. By iterating on T_w , the process is continued until the calculated bulk liquid temperature approaches satisfactorily the prescribed value (figure 2b.).

3.3 Validation on reference cases

Two reference cases, extracted from Sato's article have been chosen [2] in order to validate our numerical code. Their characteristics are summed up in Table 1. Both of them are related to air/water bubbly flow:

- Case 1 (C1): adiabatic two-phase bubbly flow,
- Case 2 (C2): heated two-phase bubbly flow.

Figure 3 shows comparison between profiles calculated by our code and those calculated by Sato, [2], for both cases. Experimental profiles measured by Sato are also represented for liquid velocity and temperature. One can observe that the agreement is good. We should also mention that our model calculate the mixture velocity instead of the liquid velocity. Nevertheless, as the pressure and the void fraction are low ($\rho_G \ll \rho_L$ et $\alpha_G \ll 1$), those two velocities are very close.

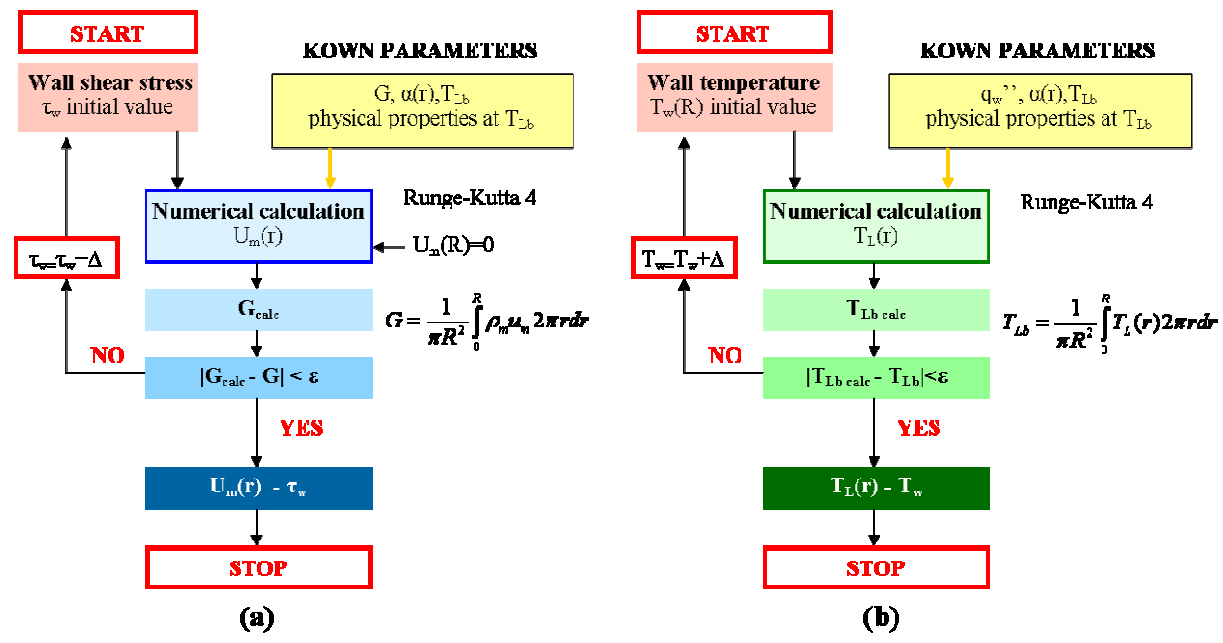


Figure 2 Diagrams for the calculations of (a) Velocity distribution – (b) liquid temperature distribution

		T _{Lb} °C	P Mpa	J _L m/s	G kg/m².s	ρ _L kg/m ³	$ ho_{ m G}$ kg/m ³	$v_{\rm L} \\ m^2/s \\ x10^{-7}$	k _L W/m.K	C _{pL} J/kg. K	U _b m/s	d _b mm	D mm	q _w '' kw/m
ſ	C1	30	0.115	0.5	498	995.6	1.29	8.01	-	-	0.2	4.8	26	-
ſ	C2	13.6	0.115	0.93	930	999.3	1.22	11.81	0.5867	4190	0.2	4	16.9	118

Table 1 Flow parameters for the reference cases

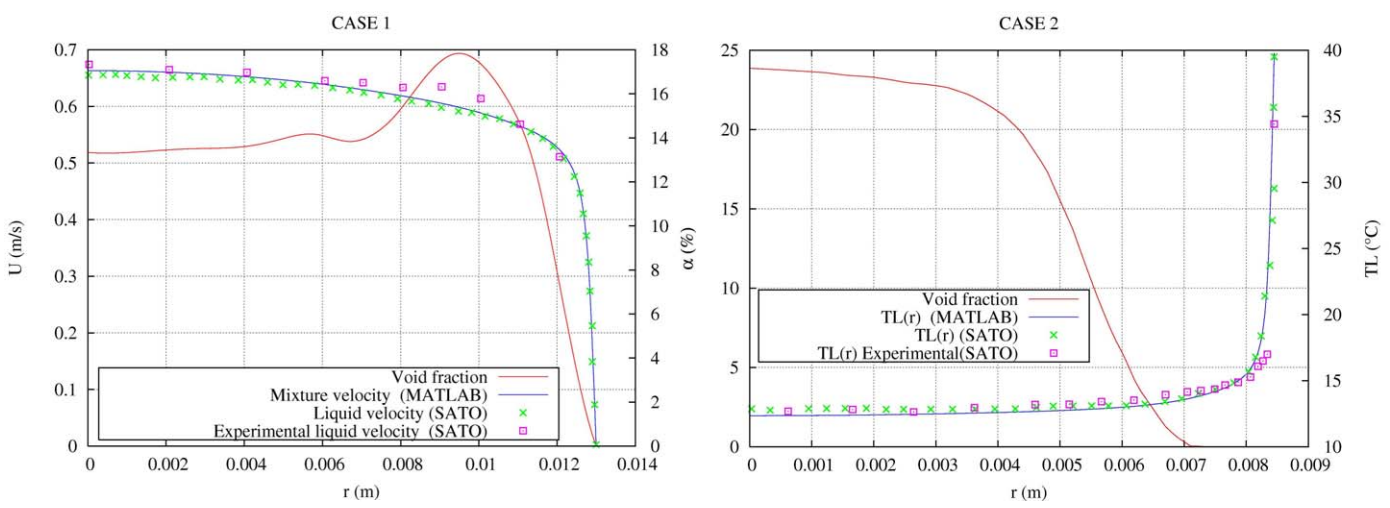


Figure 3 Comparison of the predicted profiles by Sato, our Matlab code and experimental data for velocity and liquid temperature

	⟨æ⟩ Sato %	<α> Matlab %	τ _w Sato Pa	τ _w Matlab Pa	τ _w exp Pa	Tw Sato	T _w Matlab °C	T _w exp °C
C1	13.1	13.09	1.47	1.444	2.14	-	1	-
C2	9.7	9.54	-	3.295	-	39.2	39.77	34.6

Table 2 Flow parameters measured and calculated by Sato and Matlab code These tests validate our numerical tool and allow us to extent it on boiling data.

4. The experiment DEBORA

In order to reproduce the same flow characteristics as water in PWRs conditions but for much lower pressures and heat fluxes, **R12** has been used in experimental device DEBORA (Garnier *et al.*, [3]). This experiment deals with local measurement in a R12 high pressure boiling two-phase flow by means of a two sensors optical probe coupled with a thermocouple (Ø 0.5mm). The test section is a 3,5m long heated tube with an inner diameter of 19,2 mm. The probe is located at the end of the heated length and can be moved along a diameter (figure 4) to perform some measurements.

The control parameters of the loop are the exit pressure P_e , the mass velocity G, the heat flux Φ and the inlet equilibrium quality $x_{eq,in}$. Void fraction, gas velocity and liquid temperature radial profiles are measured.

The equivalent conditions relating water to R12 experiments are based on five scaling criteria:

- Identical geometry,
- Same vapour/liquid density ratio to scale the corresponding pressure P:

$$\left(\frac{\rho_L}{\rho_G}\right)_{water} = \left(\frac{\rho_L}{\rho_G}\right)_{R12}$$
(30)

- Same Weber number to determine the corresponding mass flux G:

$$\left(\frac{G^2 D}{\rho_L \sigma}\right)_{water} = \left(\frac{G^2 D}{\rho_L \sigma}\right)_{R12}$$
(31)

where L is the heated length, D the tube diameter and σ the surface tension.

- Same boiling number to calculate the corresponding heat flux Φ :

$$\left(\frac{\Phi}{Gh_{LG}}\right)_{water} = \left(\frac{\Phi}{Gh_{LG}}\right)_{R12}$$
(32)

where h_{LG} is the latent heat of vaporization.

- Same equilibrium inlet quality to determine the equivalent inlet temperature:

$$x_{eq,in} = \frac{h_{L,in} - h_{L,sat}}{h_{LG}} \tag{33}$$

where $h_{L,in}$ is the liquid inlet specific enthalpy and $h_{L,sat}$ is the specific enthalpy of saturated liquid.

The similarity criteria lead to the R12 equivalent conditions of Table 3.

Control parameters	Water	R12
Exit pressure (MPa)	10-18	1.4-3.0
Mass flux (kg/m².s)	1000-5000	1000-5000
Heat flux (MW/m²)	0.5-6.5	0.05-0.65
Inlet temperature (°C)	50-320	20-80
Equilibrium exit quality	-0.15+0.15	-0.15+0.15

Table 3 Water operating conditions and corresponding R12 flow characteristics

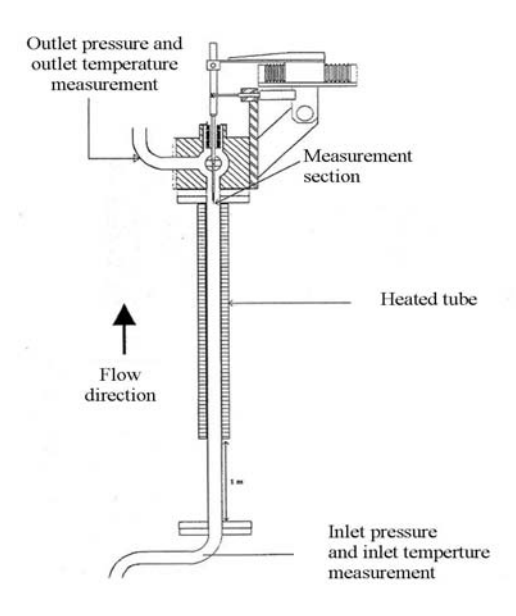


Figure 4 The measurement section DEBORA

5. Comparison of the model with the experimental DEBORA data

The purpose of this section is now to compare experimental measurements performed on DEBORA loop with the results obtained with the model previously described in Section 2.

5.1 Test cases chosen

As large numbers of tests have been realized on the data bank DEBORA, we have selected 4 cases (Table 4), whose thermohydraulic conditions covers the experimental domain explored on DEBORA. Thermal and physical liquid properties are calculated at bulk liquid temperature (\approx T_{sat} for the Test 1 and 2) and vapor ones are calculated at T_{sat} (Table 5).

	Quantity of interest	Number of phases (Single/Two)	P _e Bar	G kg/m².s	Φ Kw/m²	T _{L,e} ∘C	X _{eq,exit}
TEST 1	Gas velocity	T	14	2022	74	31.39	-0.00434
TEST 2	Gas velocity	T	14	2009	78	33.94	0.02557
TEST 3	Liquid temperature	S	26	5013	74	40.59	-0.4837
TEST 4	Liquid temperature	T	26	1983	74	70.31	0.0806

Table 4 Flow parameters for the test cases

		T _{Lb} °C	T _{sat} °C	ρ _L kg/m³	ρ _G kg/m³	$\begin{array}{c} \upsilon_L \\ m^2/s \\ x10^{-8} \end{array}$	k _L W/m.K	C _{pL} J/kg.K	σ N/m	U _b m/s	D _b mm
T	EST 1	-	56.21	1181.8	82.55	9.7	-	-	0.00493	0.0817	0.815
T	EST 2	-	56.21	1181.8	82.55	9.7	-	-	0.00493	0.0618	0.986
T	EST 3	50.93	86.47	1222.7	-	12.1	0.0596	1051.4	-	-	-
T	EST 4	86.34	86.47	1020.7	172.51	8.85	0.0459	1406.8	0.00177	0.0477	0.456

Table 5 Physical and thermal properties of fluids (R12)

5.2 Velocity distribution

5.2.1 How to express u_g from u_m ?

As on DEBORA, only the gas velocity is measured, we propose to use a method to deduce u_g from mixture velocity u_m distribution calculated by the model. Noticing that the calculated mixture velocity u_m and the measured gas velocity u_g profiles present similar shapes, we propose as a first step to express u_g and u_l as follows:

$$\begin{cases} u_g(r) = U_{g,MAX} f(r) \\ u_l(r) = U_{l,MAX} f(r) \end{cases}$$
(34)

where f(r) is a profile function defined as:

$$f(r) = \frac{u_m(r)}{U_{m MAX}} \tag{35}$$

 $U_{\text{g,MAX}}$ is obtained from experimental data using a method of least squares regression. $U_{\text{l,MAX}}$ is deduced from the mass balance equation.

5.2.2 <u>Velocity profiles</u>

Figure 5 presents the results obtained for cases 1 and 2. For each test we have plotted the void fraction profile, the calculated mixture velocity profile, the deduced gas velocity profile using equation (34) and the experimental gas velocity profile.

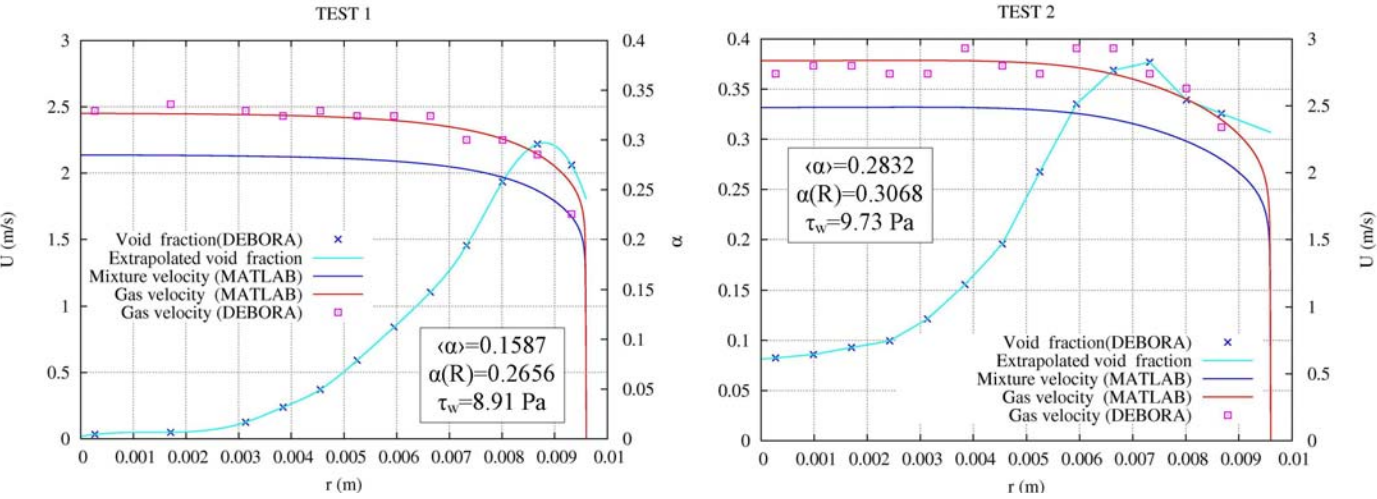


Figure 5 Comparison of gas velocity distributions

As we can see on the figure 5, the agreement between experimental measurements and the model calculation is good according to the uncertainty of velocity measurements ($\Delta V/V \approx 10\%$, Garnier *et al.* [3]).

This result is even more significant because much more DEBORA's tests have been calculated on a large range of experimental data (from sub-cooled to saturated flow with $<\alpha>$ as large as 40%) and the result of the comparison with data remains satisfactory. In order to integrate equation (28), it is necessary to know the value of τ_w . Unfortunately, this parameter has not been measured during DEBORA's experiments. That explains it has been necessary to use an iterative scheme for solving equation (28), by increasing τ_w and calculating the associated mixture velocity until the calculated velocity is consistent with the imposed mass flow rate on the test section. In fact the model calculates a couple of parameters (τ_w , τ_w), consequently the consistency of τ_w with data may result of an error on τ_w which has not been measured on DEBORA. In order to validate the couple (τ_w , τ_w), we have compared the calculated value of τ_w to Friedel's model [7], developed for fluids such as R12, for a range of parameters including DEBORA's conditions. Table 6 compares the wall shear stress obtained with the code and with Friedel's correlation. It can be observed a relative deviation less than 10% which agrees with the known uncertainty of the correlation.

	τ _w (MATLAB) – Pa	τ _w (FRIEDEL) - Pa
TEST 1	8.91	8.77
TEST 2	9.73	10.43

Table 6 Wall shear stress calculated by numerical resolution and by Friedel's Correlation

5.2.3 Discussion

If the result of this comparison appears to be positive, it does not completely prove the relevance of the model. Nevertheless it can be concluded that the model of Sato, established for two-phase bubbly flows, seems to give a good description of **transfer process of momentum in high pressure convective boiling two-phase flows.**

5.3 Temperature distribution

Contrary to τ_w , the heat flux q_w " is a known parameter which is measured in DEBORA's experiment. Consequently solving of equation (29) gives the only one unknown parameter, the liquid temperature profile. This profile can be directly compared to the experimental data.

5.3.1 Comparison of the profiles

It is necessary to distinct the two chosen tests (Tests 3 and 4). Indeed, Test 3 corresponds to a heated single-phase flow whose equilibrium exit quality is lower than -0.4 while Test 4 corresponds to a saturated boiling two-phase flow with a high equilibrium exit quality. Figure 6 presents the results obtained for both tests. For each of them we have plotted the experimental and calculated liquid temperature profiles. For Test 4, the void fraction profile and the saturation temperature are added on the plot.

5.3.2 Discussion

Figure 6 reveals two distinct behaviors. For the Test 3 which corresponds to single-phase flow, the agreement between experiment and calculations is excellent. This result is not surprising because the model of Sato used on this test is reduced to a simple mixing length model with a Prandtl analogy.

On the opposite, Test 4 reveals significant discrepancies between the model and the measured liquid temperature profiles. Indeed, the experimental temperature profile stays about saturation temperature whereas the model predicts a sharp increase of the temperature in the region close to the wall (T_w is overrated of 30°C). Same results have been observed for all the tested boiling cases.

Such a behavior is obviously incoherent because for boiling flows and for such thermalhydraulics conditions, the over heating at the wall should be of an order of magnitude of 1 or 2°C (Garnier *et al.*, [3]).

According to us, two reasons may possibly explain the observed discrepancies. Overrating the wall temperature means an efficient mechanism of heat evacuation is missing. At section 2.2, it is supposed that wall heat is only transported by liquid phase.

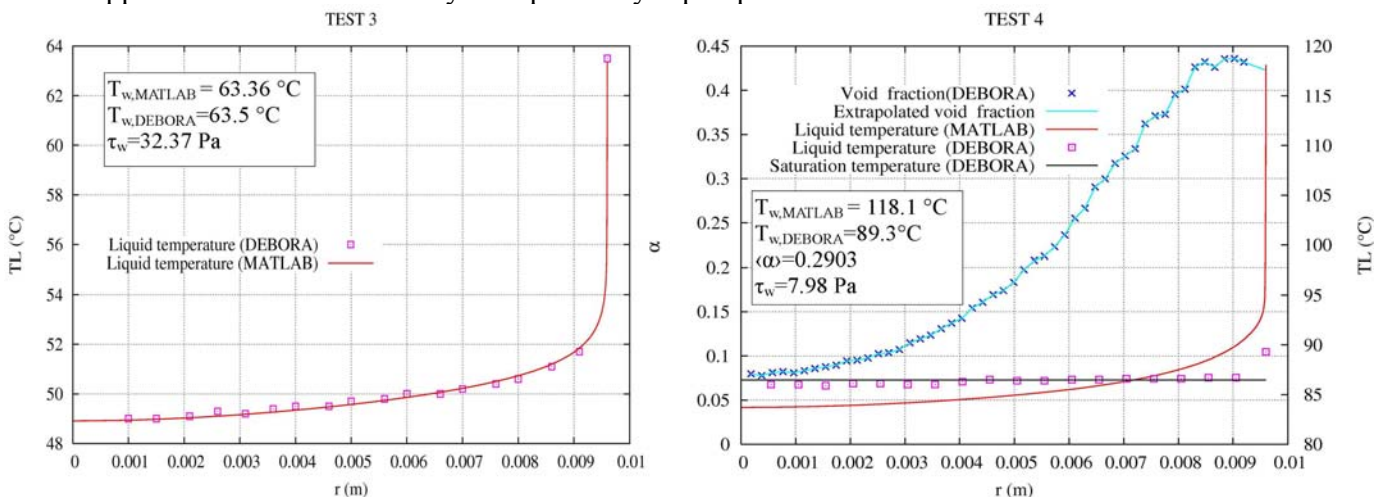


Figure 6 Comparison of liquid temperature distributions

If this is obvious in single-phase turbulent flow, the contribution of the gas phase to energy removal is significant in boiling flow especially at the vicinity of the wall, where bubbles are created. A second arguable hypothesis is the Prandtl analogy ($\varepsilon_M = \varepsilon_H$), which is obviously valid for single-phase flow but not yet proved to be valid for boiling flows.

6. Conclusions

A theory for momentum and heat transport in two-phase bubbly has been proposed by Sato, [1], based on the assumption that turbulence may result from two contributions; an inherent liquid turbulence and a turbulence induced by bubble agitation.

In this work, the performance of this model has been tested against high pressure convective boiling flows thanks to the experimental data bank DEBORA.

First results obtained for the mechanical part of the modelling are encouraging. If we can not conclude on the relevance of this model, it seems to be sufficient to correctly describe transfer process of momentum in high pressure convective boiling two-phase flows. Such results seems to validate the main assumptions of the model that are independence of the pressure gradient from radial position, uniformity of physical fluid properties, neglectability of the convective term in momentum balance equation and quasi developed flow approximation.

For thermal aspects, comparison between the liquid temperature distributions calculated with the model and those measured on DEBORA shows some important discrepancies which are not observed on single-phase heated flow and non boiling bubbly flow. According to us such results can be explained by two possible mechanisms: the Prandtl analogy (ϵ_M = ϵ_H) and the effect of the gas phase to energy removal. We are currently working on this last effect which is according to us the dominant parameter.

To conclude beyond Sato *et al.* model, the method exposed in this paper appears as a promising way to validate turbulent models using experimental results especially for PWR's conditions.

7. References

- [1] Y.Sato, K.Sekoguchi, "Liquid velocity distribution in two phase bubble flow", *Int. J. Multiphase Flow*, 1975, Vol. 2, pp.79-95.
- [2] Y.Sato, M.Sadatomi, "Momentum and heat transfer in two-phase bubble flow", I-Theory, II-A comparison between experimental data and theoretical calculations, *Int. J. Multiphase Flow*, 1981, Vol. 7, pp.167-177.
- [3] J.Garnier, E.Manon, G.Cubizolles, "Local measurements on flow boiling of refrigerant 14 in a vertical tube", *Multiphase Sci.Technol.*, 2001, Vol 13, pp.1-111.
- [4] M.Ishii, "Thermofluid Dynamic of Two-Phase Flow", collection de la direction des Etudes et Recherches d'électricité de France, Eyrolles, 1975.
- [5] H.Reichardt, "Vollständige Darstellung der turbulenten Geschwindigkeitsverteilung in glatten Leitungen", 1951, ZAMM 22, 241-243.
- [6] M. Ishii et T. Hibiki, "Distribution parameter and drift velocity of drift-flux model in bubbly flow", International Journal of Heat and Mass Transfert 45, 2002, 707-721.
- [7] Friedel, "Improved friction pressure drop correlations for horizontal and vertical two phase pipe flow", European Two-phase Flow Group Meeting, 1979, paper E 2.